

# Effect of Miscibility and Forced Compatibility on Damping Properties of CIIR/PAC Blend

Guang Su Huang, Xiang Ru He, Jing Rong Wu, Qi Ying Pan, Jing Zhen, Zhuo Hong

State Key Laboratory of Polymer Material and Engineering, College of Polymer Science and Engineering, Sichuan University, Chengdu, Sichuan 610065, People's Republic of China

Received 8 August 2005; accepted 9 January 2006

DOI 10.1002/app.24252

Published online in Wiley InterScience (www.interscience.wiley.com).

**ABSTRACT:** In this study, a kind of novel damping materials was prepared based on the blend of chlorinated butyl rubber (CIIR) and polyacrylate (PAC) synthesized by different molar ratio of butyl methacrylate and ethyl acrylate. Research results from experiments and analyses by employing DMA, TEM, and FTIR show that whether at a cocured system or noncocured system, it can be achieved to shift a loss peak of CIIR towards a higher temperature region and to keep the damping value from markedly decreasing, which broadens the effective damping function area of CIIR to the vicinity of ambient temperature. In the former system, the thermodynamical miscibility of CIIR and PAC, to some extent, is predominated by the molecular design of PAC, while in the latter system, covulcanized networks play a more significant role in improving compatibility and abating

the peak split, though the suppression effect of thermal stress on the transition of CIIR  $T_{II}$  transition still can not be neglected. Furthermore, transition state derived from the cocuring CIIR and PAC cannot make the phase separation completely take place, and consequently results in the deformation of phase morphology of the cocured CIIR/PAC blend. It is the influence of thermodynamics miscibility and forced compatibility in different size that makes the suppression effect of foreign PAC on CIIR  $T_{II}$  transition be controllable. © 2006 Wiley Periodicals, Inc. *J Appl Polym Sci* 102: 3127–3133, 2006

**Key words:** butyl rubber; polyacrylate; blend; microphase structure; damping behavior

## INTRODUCTION

Butyl rubber, a kind of copolymer of isobutylene and isoprene, can be divided into both nonhalogenation butyl rubber and halogenation butyl rubber, the latter like chlorobutyl rubber, CIIR, and bromobutyl rubber, BIIR, being the equal important commercial products. Capability of dissipating energy and strong dependence on temperature are the striking features of butyl rubber, and this is because the molecules of butyl rubber in which every interval carbon in main carbon chain bears two methyl groups as well as its unique aggregation state in which  $T_{II}$  transition a liquid–liquid transition, occurs above  $T_g$  makes butyl rubber appear as an intense loss peak; its precise mechanics is still unclear.<sup>1–5</sup> Butyl rubber has been used as conventional damping materials; however, since the loss peak occurs at relatively lower temperature region, butyl rubber nearly loses its valid damping function in the vicinity of ambient temperature. In addition, butyl

rubber, including CIIR, still has some other deficiencies such as poor processibility, interface adhesion, oil-resistance, etc.

Many scientists have been engaged in research on the improvement of the properties of butyl rubber through employing grafting copolymerization, reactive processing, or dynamic blending with other monomers or polymers. They have achieved some successes, among which the investigations by Suma, Joseph, Shin-Ichiro<sup>6,7</sup> indicate that a compatible blending can be realized between butyl rubber and EPDA or NR, so that the processability and mechanical properties of the rubber can be markedly risen, and a loss peak broadened to lower temperature can be obtained; yet it is unfeasible to shift the transition peaks towards higher temperature region. During the course of choosing plastics with a higher  $T_g$  such as polypropylene (PP) to blend with butyl rubber, Chung et al., Kenzo et al., and Mishra et al.<sup>8–10</sup> also gained certain achievements. However, it is unexpected that the loss peak of the blend moves to lower temperature of 0°C and its intensity is also greatly decreased, as Liao et al.<sup>11</sup> revealed.

Undoubtedly, it is difficult to broaden the transition peak of butyl rubber to higher temperature region while keeping the height of the transition peak from being decreased significantly. It leads to a lot of scientific problems such as phase morphology, domain

Correspondence to: G. S. Huang (jenny\_huang2005@yahoo.com).

Contract grant sponsor: Ministry of Education Foundation and National Science Foundation; contract grant number: 10266025.

size, compatibility, and adhesion in both phase interfaces and so on during blending the second components of  $\alpha$ -olefin polymer.

Polyacrylate (PAC) molecules facilitate being tailored, for they are rich in monomers whose copolymer displays different  $T_g$  transitions with higher intensity. Chung et al.<sup>8</sup> has ever grafted MMA on IIR by using borne as catalyst, but unfortunately, the graft reaction take place only in the condition that rubber is melted. In this study, a novel ideal based on blending CIIR and PAC is first presented and realized, and then the relationships between the structures and properties of the resulting blend are intensively investigated, revealing some interesting questions.

## EXPERIMENTAL

### Materials

Chlorinated butyl rubber (CIIR), the trade name of EXXON 1086, was made by Exxon Chemicals Co. (USA). Phenol-formaldehyde resin (PR), the trade name 201, was provided by Chongqing Resin Factory (China). Acrylate monomers of ethyl acrylate (EA), butyl methacrylate (BMA), and glycidyl methacrylate (GMA) to synthesize poly(meth)acrylate (PAC) copolymer were supplied by Beijing Dongfang Chemical Industry. Other curing auxiliary agents were commercial chemicals.

### Synthesis and preparation of the sample

PAC elastomer bearing GMA vulcanizing active points or not was synthesized through a conventional emulsion polymerization method at a lower temperature of  $(25 \pm 2)^\circ\text{C}$ , according to the ratio of monomers shown as the following: At synthesis of three kinds of PAC bearing no vulcanizable functional group, the weight (wt) and molar rate (mol %) of EA and BMA is (1) EA – 10 g, 1.00 mol %; BMA – 0.0 g, 0.0 mol %; (2) EA – 6 g, 0.68 mol %; BMA – 4 g, 0.32 mol %; (3) EA – 4 g, 0.49 mol %; MMA, 6 g, 0.51 mol %, respectively.

At synthesis of four kinds of c-PAC with vulcanizable functional groups, weight (wt) and the molar rate (mol %) of GMA was 5 g and 0.038 mol % in all samples, among which the weight and molar rate of EA and BMA are (1) EA – 10 g, 1.00 mol %; BMA – 0.0 g, 0.0 mol %; (2) EA – 8 g, 0.85 mol %; BMA – 2 g, 0.15 mol %; (3) EA – 7 g, 0.77 mol %; BMA – 3 g, 0.23 mol %; (4) EA – 6 g, 0.68 mol %; BMA – 4 g, 0.31 mol %, respectively.

When the reaction was over, the PAC elastomer was obtained by breaking emulsion, coacervating, rinsing, and drying. Based on the receipt of PAC/CIIR, 30:70 or 0:100 (wt %), vulcanizing agent of phenol resin (PR) of 5 wt %, other vulcanizing auxiliary agents such as stearic acid of 1 wt %, zinc oxide of 5 wt %, and carbon

black of 20 wt %, (a covulcanizing system of c-PAC/CIIR contains the same components), Pac, and CIIR were blended on a two-roll mill at a controlled temperature of  $140\text{--}160^\circ\text{C}$  and then the blend was vulcanized at  $160\text{--}170^\circ\text{C}$  under a pressure of 5.0–10 MPa.

### Characteristics of the polymer blend sample

#### Dynamic mechanical test

A dynamic mechanical spectrometer, Q800 DMA (TA Instrument), was used to analyze and characterize the relaxation behavior of the CIIR/PAC blend under the condition of heating rate of  $2^\circ\text{C}/\text{min}$ , frequency of 1, 10, 40, 80, and 125 Hz, and a cantilever beam model. The plots of DMA employing in the article are from 10 Hz.

#### FTIR measurement

The measurement of FTIR spectra of the blend polymer was conducted on a Nicolet 560 FTIR spectrometer at a resolution power of  $2\text{ cm}^{-1}$  and 32 scans.

#### TEM observation

A transmission electron microscopy (Japan Electron Co.) was used to characterize the microphase structures of the blend polymer through ultrathin section and staining it with  $\text{OsO}_4$ .

#### Solvent extraction experiment

By using  $(\text{CH}_3)_2\text{CO}$  as the extracting solvent, the experiment was conducted in a Soxhlet extraction for 72 h. After the extraction was finished, the remaining blend was dried to constant weight under a  $70^\circ\text{C}$  vacuum condition, and then the rate of extracted PAC was calculated from the remaining blend after taking off the soluble PR according to the contrast sample.

## RESULTS AND DISCUSSION

### Damping behaviors of noncured CIIR/PAC blend

Figures 1 and 2 show the damping behaviors of CIIR and CIIR/PAC blend, among which only CIIR rubber or CIIR composition in CIIR/PAC blend is vulcanized by PR resin, whereas the PAC remains a linear molecular structure. From Figure 1, the DMA plots of vulcanized CIIR, it can be seen that two evident transitions appear on the about  $-40$  and  $-20^\circ\text{C}$ , to which  $T_g$  transition and  $T_{II}$  transition of CIIR can be attributed, respectively, according to Boyer.<sup>3,4</sup> Compared with the height of  $T_g$  transition shoulder peak, the one of  $T_{II}$  transition is much higher and bigger, which demonstrates that greater contribution towards CIIR damping capability mainly originates from  $T_{II}$  transi-

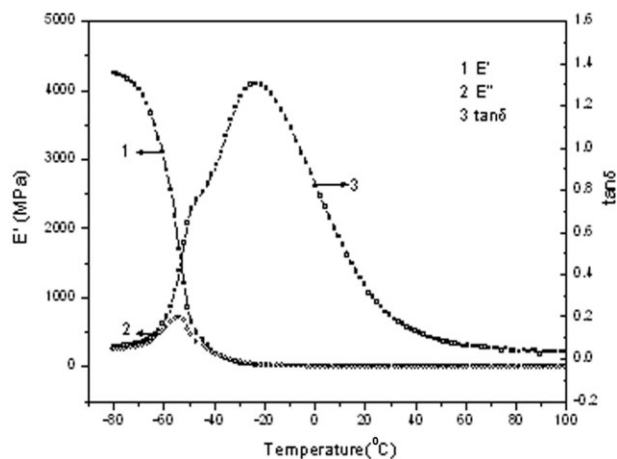


Figure 1 DMA Plot of CIIR vulcanized by PR resin.

tion of CIIR. In Figure 2, pronounced diversity in configuration of  $\tan \delta$ - $T$  curve emerges when PAc copolymer synthesized by different molar ratio of EA and BMA is blended with CIIR. At the curve 1 of CIIR/PAC  $\tan \delta$ - $T$  plot, whose PAc is synthesized wholly by EA, without BMA, a sharp and the highest shoulder peak occurs at about 15°C, regarded as the PEA transition combined with CIIR intimately. A slight peak splitting in the curve and a  $T_g$  transition of CIIR, however, still can be recognized at -20 and -40 °C respectively. By contrast, the curve 3 corresponding to CIIR/PAC blend specimen, in which BMA is 0.51M in PAc, consists of two shoulder peaks, in which one at lower temperature of -20°C should be ascribed to a contribution of CIIR composition, while the other at higher temperature of 25°C to the transition of PAc composition. In addition, the  $T_g$  transition of CIIR at -40°C is greatly weakened though some-

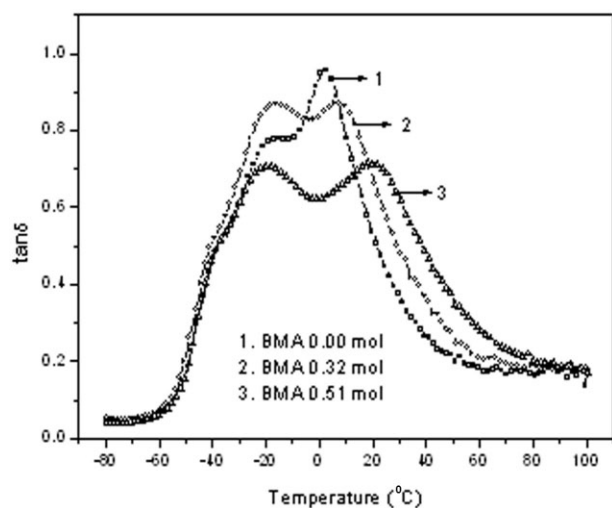


Figure 2 Curves of  $\tan \delta$  versus temperature of noncured CIIR/PAC blends.

TABLE I  
 $T_g$  of PAc Copolymers

BMA in P(EA-BMA) (mol %)	$T_g$ (°C)
0.00	-13
0.17	-8
0.23	-5.5
0.32	-3
1	+14

times it still can be recognized. What is worthy to note is that the width of the blend transition peak and the height of the  $T_{11}$  transitions of CIIR composition vary regularly according to the different molar ratio of BMA and EA composed of the PAc copolymer. As a result, it is believed that the more the content of BMA chain segments PAc contains, the deeper a valley between the two shoulder peaks and the wider the whole loss peak of the blend will be.

The cause why the phenomena occur may be interpreted on the  $T_g$  of different PAc copolymers as well as their variant compatibility with CIIR. As Table I shows, with an increased molar ratio of BMA in PAc the  $T_g$  temperature position of resulting PAc copolymer gradually rises, thus the distance between both transition of CIIR  $T_{11}$  and  $T_g$  of the PAc copolymer will change with the different molar ratio of BMA and EA composed of PAc copolymer, and at the same time the miscibility between CIIR and PAc is also dominated by varying the composition of PAc.

In the order of magnitude of the surface energy, an arrange of BMA molar ratio consisting PAc is 0.00 < 0.32 < 0.51 < 1.00, as shown in Table II. By contrast, the surface energy of unvulcanized CIIR is smaller than the vulcanized CIIR, and therefore the surface energy of the latter is closer with PAc than that of the former. In terms of the principle that the closer both of the surface energy is in a binary blend, the better homogeneity will be, it is possible that the PAc with lower surface energy has better compatibility with vulcanized CIIR. Thermodynamics is a significantly dominating factor to the miscibility of CIIR/PAC blend here, and thus the more the BMA molar ratio

TABLE II  
Surface Energy of PAc/CIIR in Different Cured System

Sample	SE (mN/N)
PAC	
BMA (mol %)	
0.00	41.0
0.32	41.8
0.51	45.9
1.00	47.3
CIIR	
Non-cured	28.2
Cured by 5 wt % PR	31.5

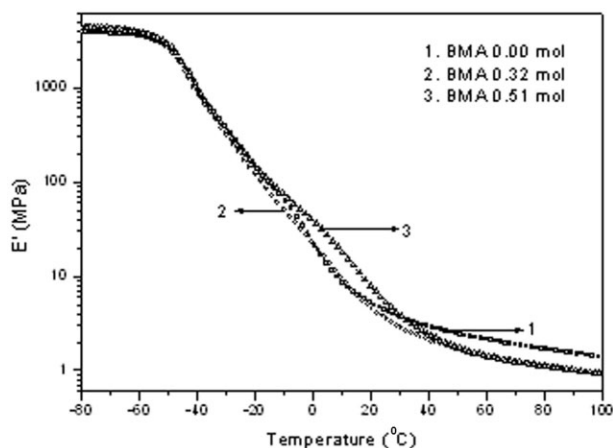


**Figure 3** Curves of store modulus versus temperature of noncured CIIR/PAC blend.

PAC copolymer contains, the poorer the compatibility will be and consequently larger split of the peak will be produced.

A decrease of the storage modulus of a noncured CIIR/PAC blend with rising temperature can be seen from Figure 3 and moreover, the samples containing more BMA segments have higher modulus in the viscous elastic state than that containing less, and it gives rise to a valley to be generated at ambient temperature range of  $\tan \delta$ - $T$  curves. However, all the blends possess enough higher storage modulus at the vicinity of room temperature, showing a reinforcing effect in the temperature range and applicability as damping materials in engineering field.

### Damping behaviors in cocured CIIR/PAC blend

Here, it should be clarified both the difference of a noncured system and a cocured system. The former only lets CIIR to be vulcanized by PR but never lets PAC to participate vulcanization. For PAC here has no vulcanizable functional groups, whereas, in the latter, the c-PAC bears vulcanizable epoxy groups, and it can be vulcanized together with CIIR by PR. What is diversity in damping performance of the CIIR/c-PAC blends from the CIIR/PAC is the second topic.

Under a cocured CIIR/c-PAC blend, influence of different compositions of c-PAC copolymer on damping behaviors is shown in Figure 4, from which it can be seen that the configurations of the transition peak of CIIR/c-PAC blend have great variety. Curve 1 shows a single peak at which the CIIR  $T_{II}$  transition hardly is recognized, for BMA composed of the c-PAC in the CIIR/c-PAC blend is equal to 0.00M, which possesses better compatibility with CIIR. However, with an increase going up to 0.17M of BMA in c-PAC copolymer, since the compatibility becomes poorer, the  $T_{II}$  transition of CIIR tends to partly separate with

$T_g$  of c-PAC, and the transition peak of the blend in curve 2 therefore is obviously broadened; on the other hand, when BMA is as high as 0.23 or 0.32M, the CIIR  $T_{II}$  transition in curve 3 and curve 4 separate from  $T_g$  transition of c-PAC, resulting in emerging of lower platform.

A comparison of the  $T_{II}$  transition in noncured CIIR/PAC blend and that in cocured blend is interesting, due to the fact that on the one hand, covulcanization greatly limits mobility of c-PAC molecules and improves its compatibility with CIIR, the deeper valley in the  $\tan \delta$ - $T$  curves is hardly observed, and therefore the peak splitting is evidently modified, and even, at the suitable condition, the peak separation can be hardly detected; on the other hand, at a noncured system, with BMA molar ratio rising, although the  $T_{II}$  transition decreases, it still can keep nearly the same height with  $T_g$  transition of PAC. On the contrary, an apparent diversity from noncured system is that the more BMA structure units in the c-PAC copolymer is, the lower the  $T_{II}$  transition peak will be, though pronounced peak splitting nearly can not be observed, which clearly indicates that  $T_{II}$  transition is very sensitive to the forced compatibility effect from cocured networks.

Figure 5 exhibits a group of storage modulus versus temperature curves of cocured CIIR/c-PAC blend. Compared with the modulus in noncured system, it can be known that the height of the loss peaks of blend  $\tan \delta$ - $T$  also tend to increase with a growth of the content of BMA content. Furthermore, the storage modulus is higher in a cocured system than that in a noncured system at the same temperature position. As a result, they respond to a relatively lower  $\tan \delta$  value.

The reason why the transition behavior of CIIR composition is so sensitive to the content of BMA segments and crosslinking networks could be inter-

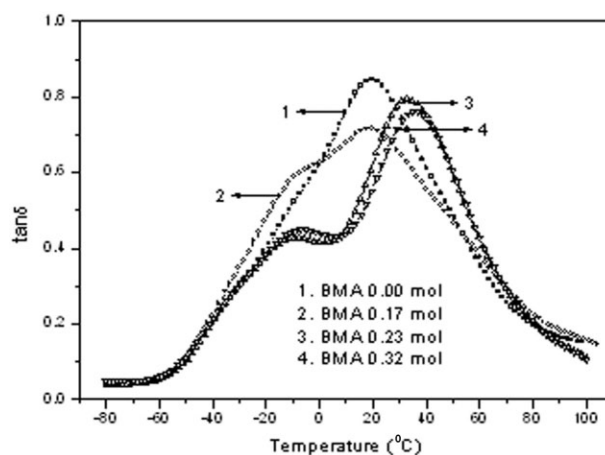


**Figure 4** The  $\tan \delta$  versus temperature curves of cocured CIIR/c-PAC blends.



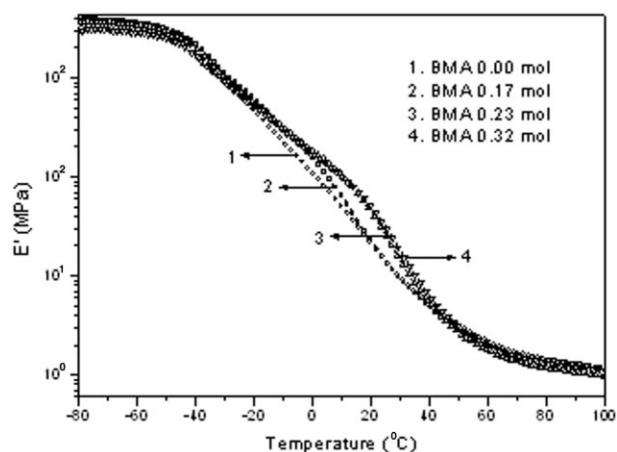


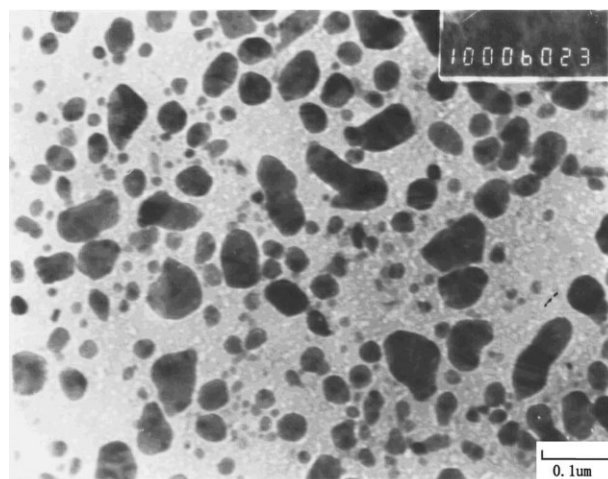
**Figure 5** Curves of store modulus versus temperature of cured CIIR/c-PAC blend.

preted from the feature of CIIR  $T_{11}$ , though it is still with arguments. Boyer<sup>3-5</sup> and others said that the  $T_{11}$  transition of CIIR derived from a retardation of CIIR macromolecular relaxation behaviors for disentanglement or other delayed movement by promissory structures. Anyhow, the liquid-liquid transition above  $T_g$  generating at the time when the sample is annealed is easy to be suppressed. The result of Liao's research has revealed that because CIIR suffers the thermal stress, its transition peak is evidently decreased when blended with PP, and consequently the  $\tan \delta_{\max}$  of CIIR/PP blend is  $\leq 0.45$  in his best result. Therefore, a too intimate contact between CIIR and PAC is unfavorable. At rising temperature, under a noncured system, where contacts of both phase of CIIR and PAC does not become relatively closer, CIIR  $T_{11}$  transition peak splits from  $T_g$  of PAC and then undertakes smaller suppression from a misfit on the behaviors of expansion and shrink between the compositions. With increased BMA structural units, the compatibility of CIIR and PAC decreases and the suppression effect slightly goes down, the height of  $T_{11}$  transition has a little decrease, but the transition peak of the blend separates heavily. However, in a cured system, where a co-crosslinking effect strengthens compatibility between c-PAC and CIIR, as a consequence, it makes the forced compatibility effect grow and both phases become closer, especially at their phase interface, and results in an increase of the suppression effect. However, the forced compatibility effect of crosslinking networks avoids a heavy phase separation and a valley producing in cured CIIR/c-PAC  $\tan \delta-T$  curve, when BMA molar ratio goes up.

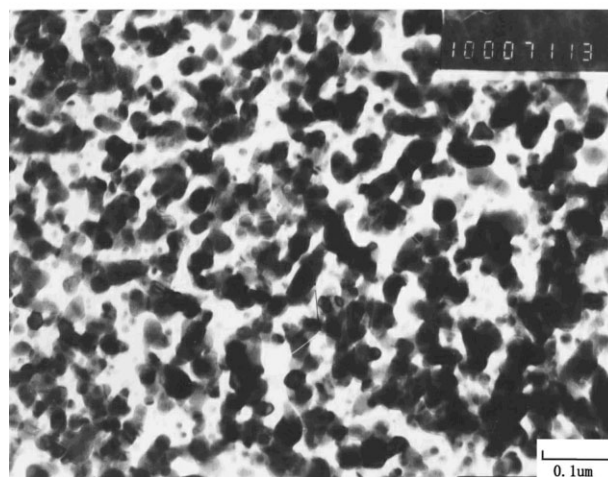
#### The microphase structures and analysis of damping behaviors

The TEM images of cured and noncured CIIR/PAC blend are shown in Figures 6(a) and 6(b), from

which pronounced variant phase morphology can be observed. At a cured system, the strained c-PAC phase displays an uninterrupted intertwining with another CIIR phase, similar to typical dual-continuous phase morphology, whereas the noncured CIIR/PAC blend exhibits monocontinuous phase morphology, where the strained PAC serves as island phase dispersing in continuous phase of CIIR, whose phase domains are 100–200 nm. What is worth of noting is that at the same ratio of CIIR/PAC, c-PAC phase in cured sample seems to occupy a bigger volume rate than that in the noncured sample. This phenomenon can be illustrated as shown in Scheme 1 and Scheme 2: at a noncured system, PAC phase-separated from CIIR continuous phase forms some independent phase domains, without linkages of chemical bonds in both polymers whose size and configuration are determined mainly by the thermodynamics miscibility of



(a)



(b)

**Figure 6** (a) The TEM image of CIIR/PEA blends. (b) The TEM image of CIIR/c-PEA blend.



**Scheme 1** An assuming pattern of molecular aggregation in noncovulcanized CIIR/PAC.

CIIR and the PAC. In view of having better miscibility between CIIR and PAC with 0M structural units of BMA, the phase separations between the binary blend is relatively complete but phase size is still smaller, at the balance condition of thermodynamics of the system. At a cocured system, origination of cocrosslinked CIIR and PAC through PR, whose action likes a bridge linking both macromolecules with chemical bones, results in a lot of media phases or transition states to be generated. It not only functions as compatibilizer to improve the interfacial tensile force of both phases, but also greatly restrains the slip of the molecules in the internal and external of the layers. Consequently, instead of independent phase patterns, some deformational dual-continuous configurations emerge in the TEM photograph of the cocured blend, there being no a complete phase separation appearing. The deformational dual-continuous patterns are believed to be a balance of phase separation of thermodynamics hindered by kinetics crosslinking effect. Furthermore, the molecules of CIIR in the transition layers are combined into strained PAC phases, which makes their phase domains to be much larger than what they are originally. As a matter of fact, a research has been reported on the crosslinking reaction between IIR and PR through forming a cyclic intermediate<sup>12</sup>, while a covulcanization system of CIIR and c-PAC by PR is our applying patent<sup>13</sup>. Number of experiments demonstrates that PR can vulcanize c-PAC, forming a novel



**Scheme 2** An assuming pattern of molecular aggregation in covulcanized CIIR/c-PAC.

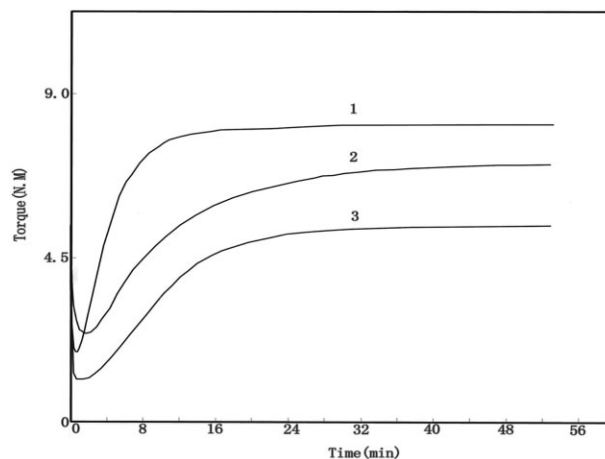


**Figure 7** The vulcanization curves of CIIR, PMAc, and CIIR/c-PMAC blend. (1) CIIR/c-PMAC blend, (2) c-PMAC, and (3) CIIR.

vulcanized system. Figure 7 is the vulcanization curves of the c-PEA, CIIR, and CIIR/c-PEA, which shows that c-PEA could be vulcanized or covulcanized with CIIR under the case that PR serves as the vulcanizator, and besides, both compositions of CIIR and c-PAC have nearly the same vulcanized rate, benefiting a vulcanizing competition and forming an easy networks in the blend. Furthermore, an effective suitable covulcanizing rate also can be gained from the novel vulcanization system. CIIR/PAC rubber cocrosslinked by PR can obtain the further evidences from following FTIR spectra shown in Figure 8, the latter has undertaken 72 h extraction at the solution of  $(\text{CH}_3)_2\text{CO}$ , which is good solution of linear PAC molecules; therefore, the existence of the characteristic absorbing peak of carbonyl group at  $1730\text{ cm}^{-1}$  is believed to be an indication of PAC participation into the covulcanization networks. Moreover, Table III supports the aforementioned results from the extract

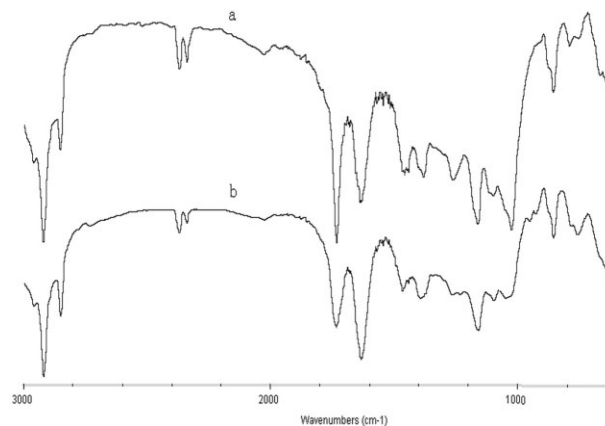


**Figure 8** The FTIR spectra of PEA and CIIR/PEA blend. (a) PEA and (b) CIIR/PEA blend..

**TABLE III**  
**Extract Content in Cocured and Non-cocured**  
**CIIR/PAC Blend**

Second composition	Extractives content (%)
C-PEA	0.06
PEA	19.7

of CIIR/PAC blend in which the second compositions are PEA bearing active vulcanizable GMA groups and bearing no vulcanizable groups, respectively, and it shows evidently the crosslinking bonds produce in cocured blend. Further characterization and research on the new vulcanization system will be reported in detail in other articles.

### CONCLUSIONS

In summary, a kind of novel damping materials can be gained by blending CIIR with PAC, regardless of employing a noncocured system or a cocured system. In both systems, the loss peaks can be shifted to a higher temperature region remarkably. Another discovery of the same significance is that a height of transition peak of the blend is predominated mainly by a miscibility derived from compositions consisting of the PAC with

CIIR and a forced compatibility effect caused by the cocured networks. Furthermore, a new vulcanized system of PAC and a covulcanized system of CIIR/PAC is first presented and primarily proved. It is believed that it is the cocured effect that causes a deformation of phase morphology of CIIR/PAC blend, and result in their displaying diverse transitional behaviors.

### References

1. Dutta, N. K.; Tripathy, D. K. *Polym Degrad Stab* 1990, 30, 231.
2. Sanders, J. F.; Ferry, J. D. *Macromolecules* 1975, 7, 681.
3. Boyer, R. F. *Order in the Amorphous State of Polymers*; Plenum: New York, 1987; 135.
4. Boyer, R. F. *J Appl Polym Sci* 1986, 32, 4075.
5. Murthy, S. S. N. *J Polym Sci Part B: Polym Phys* 1993, 31, 475.
6. Botros, S. H. *Polym Degrad Stab* 1998, 62, 471.
7. Suma, N.; Joseph, R.; George, K. E. *J Appl Polym Sci* 1993, 49, 549.
8. Chung, T. C.; Janvikul, W.; Bernard, R.; Hu, R. *Polymer* 1995, 36, 3565.
9. Kenzo, K.; Goto, S.-I.; Yamamoto, T. *J Appl Polym Sci* 1999, 74, 3548.
10. Mishra, S.; Hazarika, M.; Chandra, R. *J Polym Plastic Technol Eng* 1999, 38, 311.
11. Liao, F. S.; Su, S. A.; Tzu, C. *Polymer* 1994, 35, 2579.
12. Latimer, R. P.; Kinsey, R. A.; Layer, B. W.; Rhee, C. K. *Rubber Chem Technol* 1989, 62, 107.
13. Chinese Application Patent 200510020175.